Spiral fibre microbend sensors

T. Yoshino
K. Inoue
Y. Kobayashi

Abstract: A spiral fibre microbend-loss sensor having definite sensing characteristics is presented. By means of single-mode-fibre embedded metal springs, strain and deformation can be measured with good linearity and reproducibility and with a large dynamic range. The effects of spring parameters (radius, pitch, length) on the sensing performances are analysed and verified experimentally. Numerical simulations for the optimum design are performed.

1 Introduction

A fibre optic microbend sensor is known as a simple and inexpensive intensity-modulation fibre sensor which can detect deformation and its related various quantities such as strain [1], pressure [2], acoustic wave [3], temperature [4], water [5], etc. [6]. A fibre microbend sensor (MBS), however, despite its appearance, has very complicated sensing performances dependent on the deformation of fibre and fibre parameters. Previous MBSs mostly rely on nonuniform deformations (e.g. sinusoidal deformation) of fibre caused by microbenders such as a pair of corrugated plates, a chain roller [7] or wire winding [8], and, moreover, employ multimode fibres for the sensing fibre so that the sensing characteristics undergo modal instability, though a modelling study was conducted [9]. Because of the complicated sensing features, most uses of the MBS have been limited to simple monitoring or on-off sensors, and so the capability of analogue sensing of MBS has hardly been put into practical use.

The purpose of this paper is to develop a microbend fibre sensor which can be used for an analogue sensor having simple and definite sensing characteristics [10]. To achieve the purpose, noticing that fibre optic microbend loss can be unambiguously treated only in the case of circularly bent single-mode fibre, we introduce a spiral-form fibre microbend sensor of single-mode fibre. In the sensor, an application of an arbitrary amount of deformation in the spiral axis

leads to a uniform change in the radius of the circularly bent fibre, so that the induced change in microbend loss can be treated in both theory and experiment.

First, the design principle of the spiral fibre MBS is presented. The effects of the spiral coil radius, pitch and gauge length on the sensing characteristics are theoretically analysed. Next, single-mode-fibre embedded metal springs are fabricated and their strain sensing characteristics are experimentally investigated and shown to be in good agreement with calculations. Good performances regarding linearity, reproducibility and dynamic range are demonstrated. Finally, simulation calculations are conducted for the optimum design of the proposed sensor.
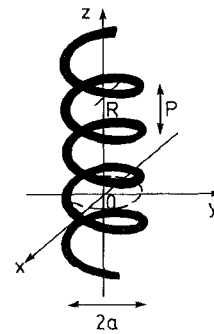

Fig. 1 *Geometry of spiral*

2 Theoretical considerations

We consider a spiral coil with pitch P and coil radius a as shown in Fig. 1. From the geometrical relationship, the spiral has a uniform radius of curvature,

$$R = a + (1/a)(P/2\pi)^2 \qquad (1)$$

If the spiral contains a pitch number n, the spring height, or a gauge length when the spiral coil is used as a sensor, is

$$L_g = nP \qquad (2)$$

and the total spiral length is

$$L = n[(2\pi a)^2 + P^2]^{1/2} \qquad (3)$$

As is given by eqn. 1, the radius R of curvature of the spiral is larger than the coil radius a. Reducing the total length of the spiral in terms of circles of radius R, the spiral involves the following turns of the circle:

$$N = L/(2\pi R) = n/[1 + (P/2\pi a)^2]^{1/2} \qquad (4)$$

which is smaller than n.

When a deformation d or a strain ε is applied to the

spiral in its axial direction, both the pitch P and the coil radius a are changed by εP and $\varepsilon' a$, respectively, in relationship with

$$\varepsilon' = -F\varepsilon \qquad (5)$$

and

$$F = [P/(2\pi a)]^2 \qquad (6)$$

which are calculated from eqn. 3 under the condition of L = constant. The stress-induced axial deformation of the spring gauge length is then

$$d = \varepsilon L_g = \varepsilon n P \qquad (7)$$

and the accompanying changes in R and N are

$$d(1/R)/d\varepsilon = -(1/a)/[1 + (2\pi a/P)^2] \qquad (8)$$

$$dN/d\varepsilon = -n(P/2\pi a)^2/[1 + (P/2\pi a)^2]^{1/2} \qquad (9)$$

Letting the transmittance of one-turn in-plane circular fibre of radius R be $f(1/R)$ and assuming that it also applies for a spiral coil having $N = n$, then the transmittance of the spiral fibre becomes

$$T(1/R) = f^N(1/R) \qquad (10)$$

The modulation index of transmittance against applied strain is given, from eqn. 10, by

$$m = dT/d\varepsilon/T$$
$$= dN/d\varepsilon \cdot \log f(1/R)$$
$$+ Nf^{-1}(1/R) \cdot d(1/R)/d\varepsilon \cdot df(1/R)/d(1/R) \qquad (11)$$

and the corresponding transmittance change is

$$\Delta T = mT = mf^N(1/R) \qquad (12)$$

Both the quantities m and ΔT are associated with the measurement sensitivity of spiral fibre MBS and are desired to be larger to achieve greater sensitivity. From eqns. 8–12 it is known that the sensitivity parameters m and ΔT, under given spiral parameters of a, P and n, can be specified only if the function $f(1/R)$ is known. Eqn. 11 of m consists of two positive terms and increases in proportion to N and hence n. On the other hand, from eqn. 12, ΔT takes its maximum at a suitable value of N and hence n.

3 Design and experimental study

3.1 Transmittance characteristics

To know the function $f(1/R)$ exactly in real fibres, we measured the transmittances of in-plane circularly bent fibres with different radii R and different turn numbers n. In the experiment, the fibre was tightly wound around metal cylinders of various radii in various turns. The cladding mode of the fibre was stripped by index-matching oil in front of the bent part of the fibre. The light source was a multimode laser diode (λ = 780 nm) to avoid undesirable interference effects, and the detector was a PIN photodiode. The fibre transmittance T was measured for both a single mode of 6 μm-diameter core, 125 μm-diameter cladding and a multimode fibre of 50 μm-diameter core, 125 μm-diameter cladding. The measured results of $-\log T$ against n are shown in Figs. 2 and 3 for the single- and multimode fibre cases, respectively. It is seen that the bend loss obeys the multiplication law (eqn. 10) with respect to coil turn number $N = n$ in the case of the single-mode fibre but does not in the case of the multimode fibre, in which the bend loss is affected by modal distribution. Thus, single-mode fibre is suited

for the present study, but not multimode fibre. Fig. 4 shows the measured single-mode-fibre transmittance function $f(1/R)$ as a parameter of coil number n. In the following calculation, it is assumed that the results of Fig. 4 apply also in spiral fibres with $N = n$. The validity of this assumption was experimentally verified within a deviation of 5%, in the region of $0 < 1/R < 0.25\,\text{mm}^{-1}$ for $n \le 5$.
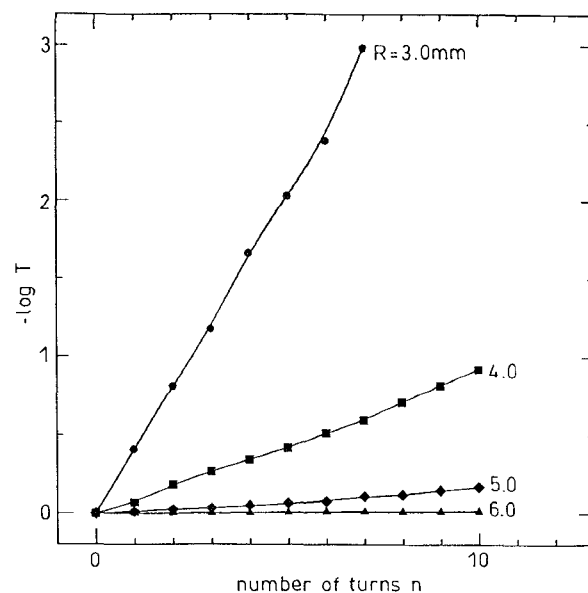
Fig. 2 *Measured dependence of transmittance T on turn number n for various radii R in single-mode-fibre coil*
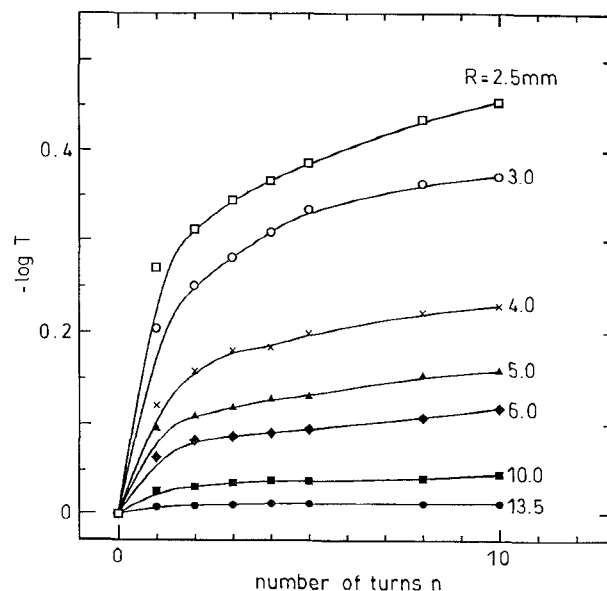
Fig. 3 *Measured dependence of transmittance T on turn number n for various radii R in multimode-fibre coil*

3.2 Sensor design and construction

The modulation index m of the sensitivity parameter increases in proportion to the spiral pitch number n and hence gauge length $L_g = nP$ for a constant pitch P. The magnitude of m for $n = 1$ is calculated from eqns. 8–11 using the function $f(1/R)$ of Fig. 4 and is shown in Fig. 5 as a function of spiral coil radius a. The m-value rapidly increases with decreasing a and P so that, to increase m, possibly large n and possibly small a and P are desirable. Practically available magnitudes of a and

146

P, however, are restricted by the durability of bent fibres and/or by the elasticity limit of the spring material. Considering this, some different types of spiral fibre MBS listed below were constructed:

Sensor I: 0.6mm-diameter piano wire spring; a = 2.6mm, P = 12mm (hence R = 4.0mm).

Sensor II: 0.6mm-diameter piano wire spring; a = 3.0 mm, P = 13mm (hence R = 4.4mm).

Sensor III: 'FIMT' of 1mm-diameter 0.6mm-thick stainless steel; a = 2.6mm, P = 7.5mm (hence R = 3.2mm).

In fabricating sensors I and II, the single-mode fibre was bonded on the ready-made spiral piano wire with increasing pitch numbers n from one to a few tens. Sensor III was constructed by using a commercially available metal-jacket fibre 'FIMT', in which a single-mode fibre is built in the steel pipe with a gelatin cushion. The FIMT was shaped into a spiral by hand without thermal processing.
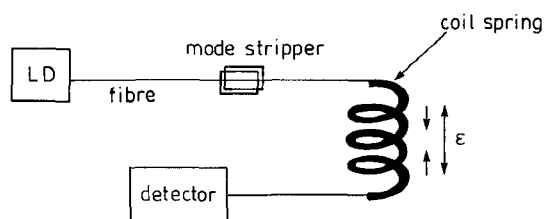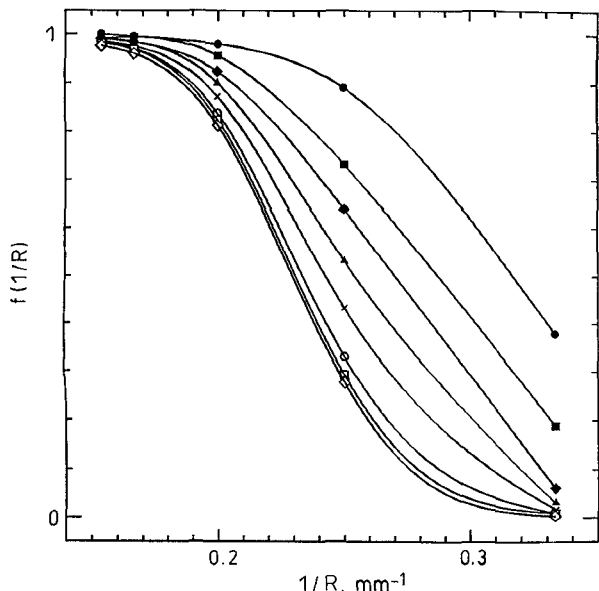

Fig. 4 *Measured transmittance function $f^n(1/R)$ against radius of curvature of single-mode fibre in-plane circular coil for various turn numbers n*
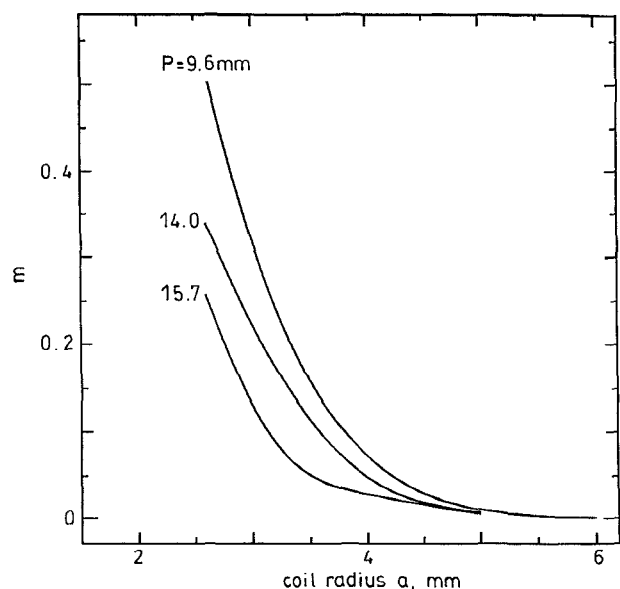n = ● 1 ■ 2 ◆ 3 ▲ 4 × 5 ○ 6 □ 7 ◇ 8

Fig. 5 *Calculated dependence of modulation index m on coil radius a for different pitches P in one-turn spiral fibre sensor*
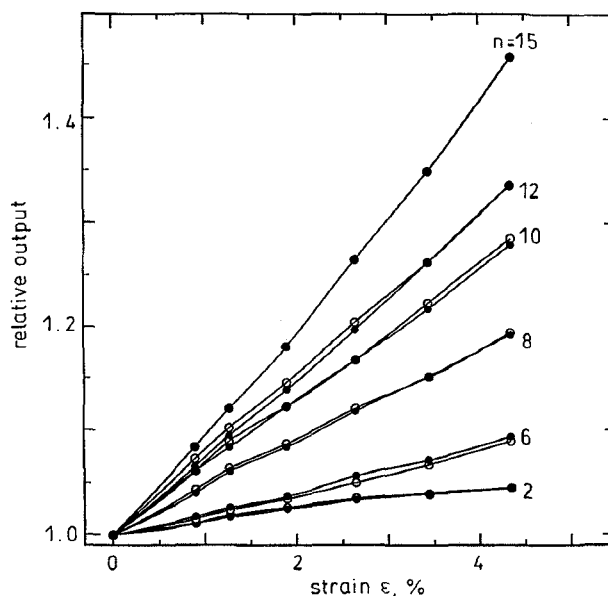n = 1

Fig. 6 *Schematic diagram for spiral fibre microbend sensors*

Fig. 7 *Measured dependence of photodetector output on applied strain ε for different pitch numbers n in spiral fibre microbend sensor I for twice experiments*
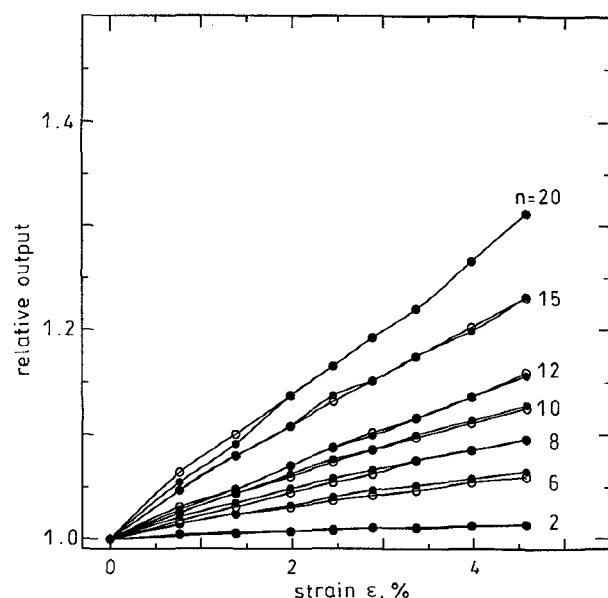a = 2.6mm; P = 12.0mm; R = 4.0mm
○ 1st ● 2nd

Fig. 8 *Measured dependence of photodetector output on applied strain ε for different pitch numbers n in spiral fibre microbend sensor II for twice experiments*
a = 3.0mm; P = 13.0mm; R = 4.4mm
○ 1st ● 2nd

3.3 Sensor characteristics

Fig. 6 shows the schematic diagram for the strain/deformation sensor. The light source and the detector were the same as described in Section 3.1. In sensors I and II, expansion characteristics were studied because reproducible uniform axial elongation could be given to the spring by pulling it with various weights. The fibre transmittances were measured as a function of

applied strain ε for different pitch numbers n, and the measured results are shown in Figs. 7 and 8 for sensors I and II, respectively. A very good linearity against applied strain is obtained for both the sensors. A very good reproducibility between two-times experiments is also observed. The strain sensitivity increased with an increase in the pitch number n. The dynamic range ε_{max} was about 4%, governed by the elasticity limit of the metal spring used. The corresponding maximum deformation is $d_{max} = \varepsilon_{max} nP$, which is, for example, 7.2mm for sensor I with $n = 15$. Thus, in strain or deformation measurement, a large dynamic range with linear scale was demonstrated. The resolution is affected by the mechanical instability of the spring motion and the output light power instability. The resultant instability of the sensor system was less than 1%.
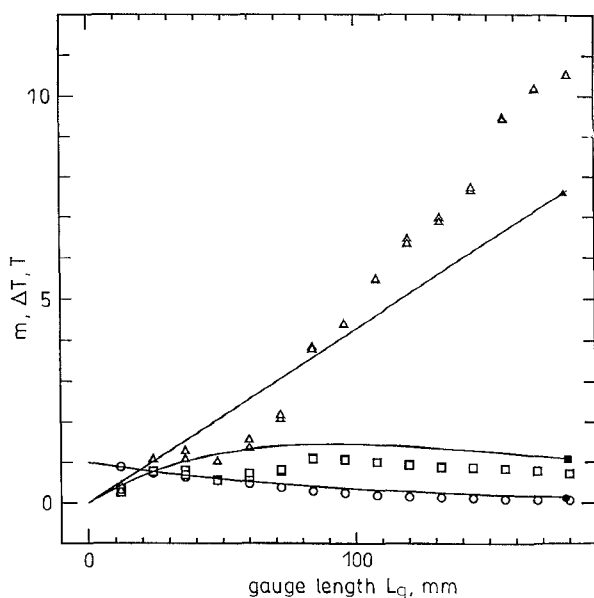
In both sensors I and II with various gauge lengths $L_g = nP$, the modulation index m, the corresponding transmittance change ΔT and the transmittance T are measured as a function of applied strain ε. The measured results are shown in Figs. 9 and 10, together with the calculations of eqns. 10–12. In both sensors, fairly good agreement between the measured and calculated results is obtained regarding m, ΔT and T. Some deviation of the experimental results from the theory is expected because the fibre was not uniformly bonded on the spiral wire on account of the hand working. In both sensors I and II, m could take over 1 and ΔT became almost 10. The maximum ΔT occurred at gauge lengths L_g of ~100mm and 140mm for sensors I and II, respectively, in good agreement with the theoretical results.
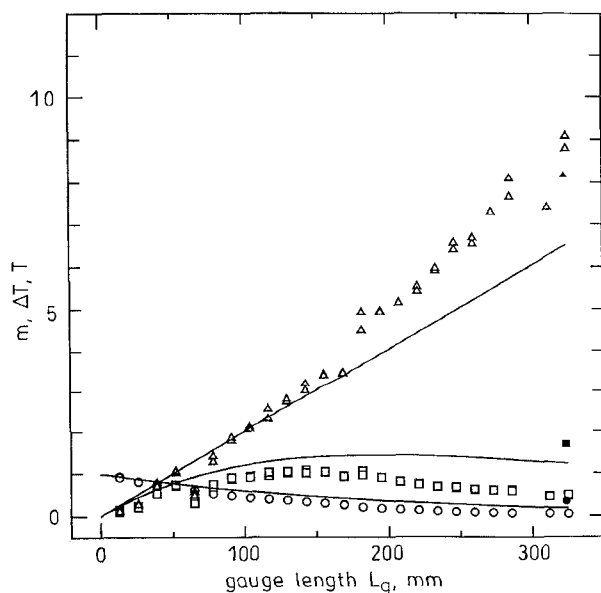

Fig.9 Dependences of modulation index m, transmittance change ΔT and transmittance T on gauge length L_g in spiral fibre microbend sensor I
$a = 2.6$mm; $P = 12.0$mm; $R = 4.0$mm
——— calculated; $\triangle$ m, $\square$ ΔT, $\bigcirc$ T, measured
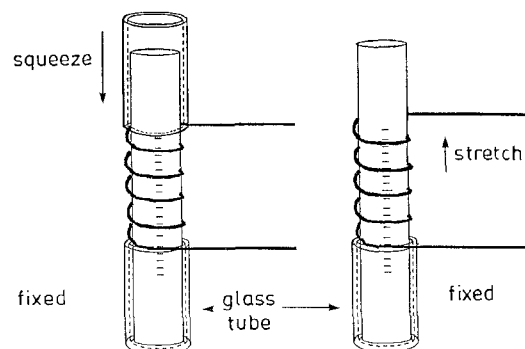

Fig.11 Diagram for squeezing and stretching a fibre-built-in metal spring
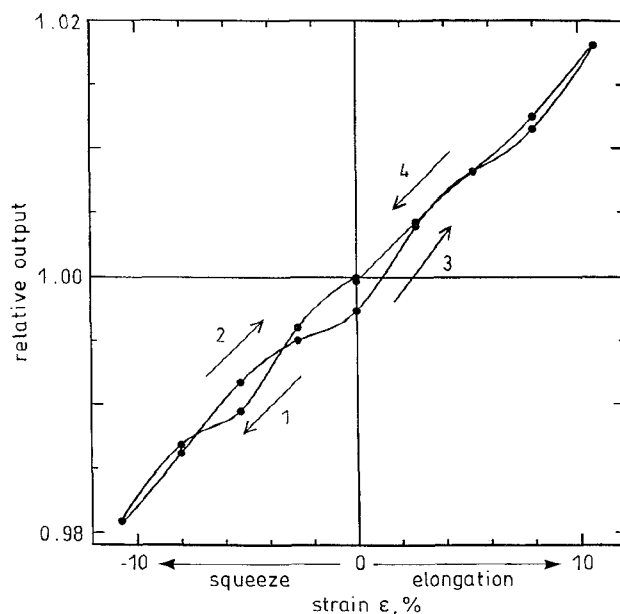
Fig.12 Measured dependence of photodetector output on applied strain ε in spiral fibre microbend sensor III

Fig.10 Dependences of modulation index m, transmittance change ΔT and transmittance T on gauge length L_g in spiral fibre microbend sensor II
$a = 3.0$mm; $P = 13.0$mm; $R = 4.4$mm
——— calculated; $\triangle$ m, $\square$ ΔT, $\bigcirc$ T, measured

For the practical sensor, the use of a fibre-built-in spring would be convenient. Sensor III was constructed by using the commercially available metal-jacket fibre 'FIMT' with $n = 5$. Both elongation and squeezing were applied to the spring in the manner shown in Fig. 11, in which a glass cylinder was inserted in the inside of the spring coil for carrying out its stable axial deformation. The measured strain characteristics are shown in Fig. 12. The sensor could detect both ± strains over a large dynamic range of 10% strain. Some hysteresis was observed, being attributable to the

imperfectly reproducible deformation of the hand-made spring. Other spiral MBSs are also constructed using metal tubes, in which the single-mode fibre was inserted and fixed by a chemical bond. Their strain characteristics were measured and showed appreciable or little hysteresis, depending on the samples constructed, indicating that the MBS very faithfully responds to the real deformation of the fibre.

To study the polarisation effect, the transmittance of an in-plane fibre coil ($R = 3$mm) was measured when its bend plane was rotated around the fibre axis, but no appreciable change was observed, as typically shown in Fig. 13.

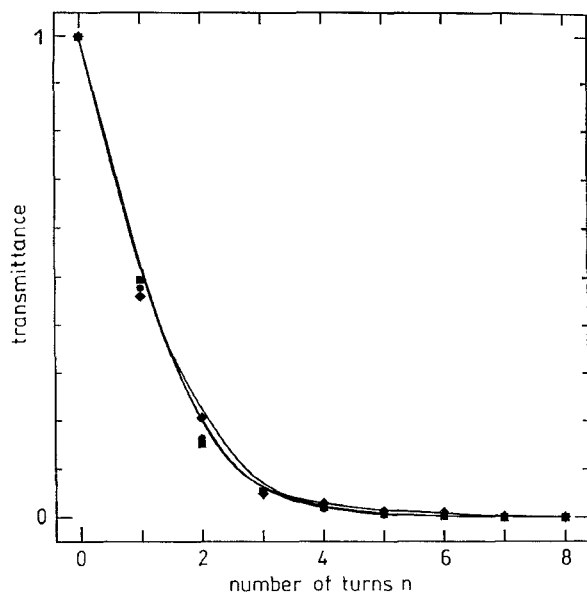**Fig. 13** *Measured polarisation dependence of transmittance of in-plane fibre coil of radius $R = 3mm$ as a function of turn number n for three different angles of orientation of fibre bend plane*
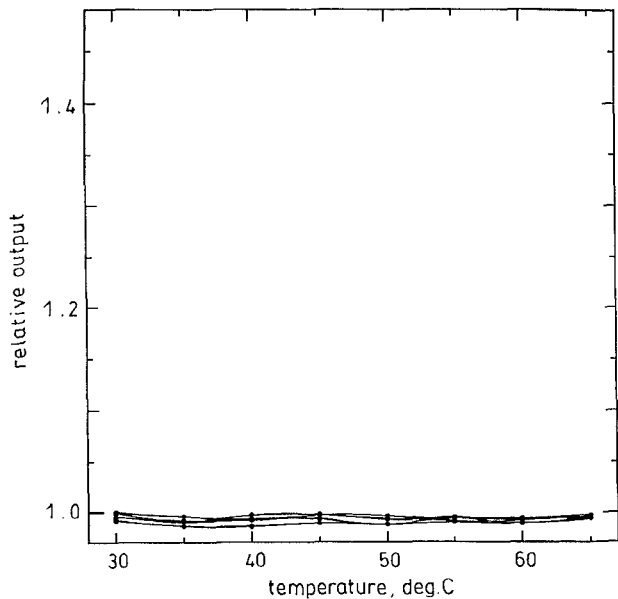● 0° ■ 45° ◆ 90°

Fig. 14 *Measured temperature dependence of metal spring fibre microbend sensor*
$a = 2.6$mm; $P = 12.0$mm; $R = 4.0$mm; $n = 10$

The temperature dependence of sensor I with $n = 10$ was tested in a temperature range between 30 and 75°C, but no appreciable change was observed, as

shown in Fig. 14; the piano wire used has a low thermal expansion coefficient of 1×10^{-6}/degree C.

4 Simulation study

As good agreement between experiment and calculation has been demonstrated, a computer simulation study would be useful for the optimum design of the spiral sensor. To evaluate the effect of spiral coil radius a, simulation calculations for different a-values from 2.6 to 5.0mm were conducted using eqns. 11 and 12 subject to the function $f(1/R)$ of Fig. 4. Figs. 15–18 show the calculated results for m and ΔT as a function of gauge length L_g, respectively. It is seen from Figs. 15 and 16 that, for a constant P, the modulation index m becomes very large for sufficiently small a, increasing with increasing L_g as well. For example, with $P = 6.4$ mm and $L_g = 500$mm, the values of m are 12500, 250 and 6.0 for $a = 2.6$, 3.0 and 4.0mm, respectively. By contrast, the transmittance changes ΔT, resulting from the product of m and T (total transmittance), are much less sensitive to a-values, as seen from Figs. 17 and 18. For example, with $P = 15.7$mm and $L_g = 500$mm, the ΔTs are 4.3, 2.3 and 0.65 for $a = 2.6$, 3.0 and 4.0mm, respectively. Furthermore, for a given P, there is an optimum gauge length $L_{g.opt}$ for maximising ΔT, and both ΔT_{max} and $L_{g.opt}$ increase with increasing P; for example, with $a = 2.6$mm, ΔT_{max}s take 0.8, 1.5, 2.4 and 4.6 at $L_{g.opt} = 20$, 100, 250 and 700mm, respectively.
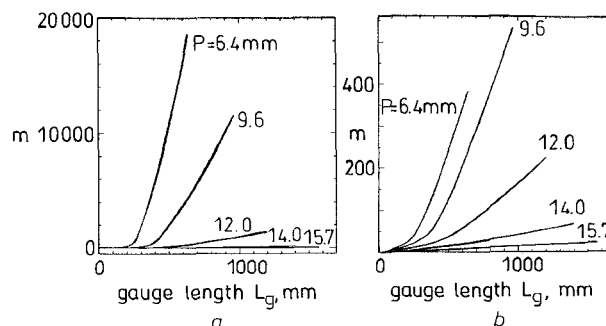

Fig. 15 *Calculated dependence of modulation index m on gauge length L_g as a parameter of pitch P for coil radii 2.6 and 3.0mm in spiral fibre microbend sensors*
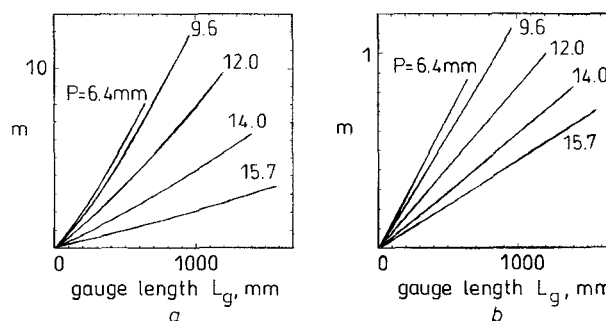a $a = 2.6$mm; b $a = 3.0$mm

Fig. 16 *Calculated dependence of modulation index m on gauge length L_g as a parameter of pitch P for coil radii 4.0 and 5.0mm in spiral fibre microbend sensors*
a $a = 4.0$mm; b $a = 5.0$mm

Besides the use of a one-point sensor, the present spiral fibre sensor has potential for multipoint sensing owing to the simple implementability of splicing to a fibre highway. Referring to Figs. 15–18, we consider one example case of $a = 4.0$mm. Then, with the use of $P = 12$mm and $L_g = 60$mm, one obtains $m = 0.5$ and $T = 0.90$, so that, with a loss penalty of 10dB, we can

149

provide 21 multiple sensors having 2.5 times higher sensitivity than that of Fig. 12. Extension to km-range continuous distributed sensing would be an interesting future research subject using the spiral fibre microbend sensor.
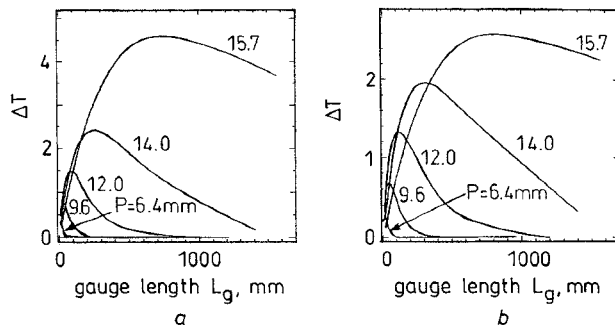

Fig. 17 Calculated dependence of transmittance change ΔT on gauge length L_g as a parameter of pitch P for coil radii 2.6 and 3.0mm in spiral fibre microbend sensors
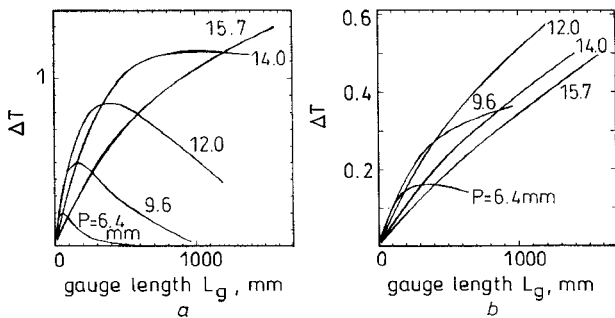a a = 2.6mm; b a = 3.0mm

Fig. 18 Calculated dependence of transmittance change ΔT on gauge length L_g as a parameter of pitch P for coil radii 4.0 and 5.0mm in spiral fibre microbend sensors
a a = 4.0mm; b a = 5.0mm

5 Concluding remarks

The developed spiral-form single-mode fibre microbend sensor uses a sensing principle based on uniform change in the bend radius of the fibre so that the sensing characteristics are definitely specified, both in theory and experiment, simply from knowledge of the circular-bend loss of the single-mode fibre. The effects of the spiral coil radius, pitch and gauge length on the sensing characteristics are theoretically analysed and experimentally verified. Good reproducibility, good linearity and large dynamic range in strain/deformation measurement are demonstrated. Simulation calculations for sensor optimisation are also conducted.

6 References

1 ASAWA, C.K., YAO, S.K., STREANS, R.C., MOTA, N.L., and DOWNS, J.W.: 'High sensitivity strain sensor for measuring structual distortion', Electron. Lett., 1982, 18, pp. 362–364
2 VARSHNEYA, D., GHERING, W.L., and BERTHOLD, J.W.: 'High-temperature fibre-optic microbend sensor'. Proceedings of 3rd Optical fiber sensors conference, San Diego, 1985, pp. 140
3 FIELDS, J.N., and COLE, J.H.: 'Fiber microbend acoustic sensor', Appl. Opt., 1980, 19, pp. 3236–3267
4 YOSHINO, T., NARA, M., and KUROSAWA, K.: 'Remote and multi-point fiber sensors using optical time domain reflectometry'. Proceedings of 13th congress of the International Commission for Optics, Sapporo, 1984, pp. 324–325
5 TOMITA, S., TACHINO, H., and KASAHARA, N.: 'Water sensor with optical fibre', J. Lightwave Technol., 1990, 8, pp. 1829–1832
6 BERTHOLD, J.W.: 'Historical review of fiber-optic sensors', J. Lightwave Technol., 1995, 13, pp. 1193–1199
7 MARVIN, D.C., and IVES, N.A.: 'Wide-range fibre-optic strain sensor', Appl. Opt., 1984, 23, pp. 4212–4217
8 OSCROFT, G.: 'Intrinsic sensors', Proc. SPIE–Int. Soc. Opt. Eng., 1987, 734, pp. 207–213
9 LAGAKOS, N., COLE, J.H., and BUCARO, J.A.: 'Microbend fibre-optic sensor', Appl. Opt., 1987, 26, pp. 2171–2180
10 YOSHINO, T., INOUE, K, KOBAYASHI, Y., and TAKAHASHI, Y.: 'Spring coil fiber microbend sensor with well-defined characteristics'. Proceedings of 11th Optical fiber sensors conference, Sapporo, 1996, pp. 264–267